ISSN 2320 2599
Volume 2, No.1, January – February 2013
International Journal of Microwaves Applications
Available Online at http://warse.org/pdfs/2013/ijma05212013.pdf

Estimation of the Electronic Efficiency of a Gyroklystron Amplifier

M. S. Chauhan[1], M. V. Swati[2], P. K. Jain[3]
Centre of Research in Microwave Tubes, Department of Electronics Engineering,
Indian Institute of Technology (Banaras Hindu University),
Varanasi–221005, INDIA.
Email: mschauhan83@yahoo.com[1], swati.mv18@gmail.com[2], pkjain_crmt@sify.com[3]

ABSTRACT

In the present paper, a generalized self-consistent single mode linear analysis of gyroklystron has been presented. The analysis has been used to estimate and optimize the electronic efficiency of the gyroklystron device. The efficiency contours, necessary for the preliminary design of a gyroklystron, have been drawn by solving the coupled equations using Runga-Kutta method for the various device parameters. Using these efficiency contours, the electronic efficiency of an experimentally reported Ka band gyroklystron operating at the fundamental harmonic mode has been estimated. The results obtained from the present analysis have been found in match with the reported experimental values within 10%. The present analysis is generalized in nature and would be useful for the initial design of the gyroklystron amplifers of any desired frequency and power.

Key words: Microwave tubes, millimeter wave amplifier, gyroklystron, beam wave interaction.

1. INTRODUCTION

In recent years, there are renewed interest and activities in developing the gyro-devices, like gyrotrons, gyro TWTs, gyroklystrons, etc. which belong to the fast-wave microwave electron beam devices family. Amongst all the gyro-devices, the gyrotron, which is a high power oscillator in the millimeter and sub-millimeter wave range, has been matured both analytically and experimentally during the last few decades primarily due to its variety of applications [1-2]. Gyroklystron, an amplifier of this family, is also emerging as one of the promising candidate due to its capabilities to provide high gain and moderate bandwidth with good linearity and phase stability in the millimeter and sub-millimeter wave regime [3]. Gyroklystrons find application in systems like high resolution radars, advanced high gradient linear particle accelerators, deep space and specialized satellite communication, etc. where high power millimeter wave amplifiers are needed.

The gyro-klystron — analogous to its slow-wave counterpart, klystron a slow wave microwave tube, is a fast wave amplifier. The resonant cavity arrangement in a gyro-klystron is similar to that in a conventional klystron for localized and intensified beam-wave interaction to produce high powers and efficiencies. The bunching of electrons is relativistic in a gyroklystron as in a gyrotron [4]. Unlike in conventional klystron, in gyroklystron, it is the electron beam rather than the interaction structure that is made periodic. Here, electrons radiate due to a phenomenon called bremsstrahlung, as they move in helical trajectories in a background magnetic field, and interact with a transverse electric mode of a circular cavity. In such type of a device, the radiation wavelength is determined by the background magnetic field rather than by the size of the interaction structure. Due to this reason gyroklystron can be operated at the higher frequencies with increased transverse dimensions which in turn increase their power handling capability at millimeter and sub-millimeter wave frequencies.

In the family of gyro-devices, the gyroklystron amplifiers are still at the development stage and have not reached to the status of a matured device. Analytical research led to the considerable physical insight into the principle of operation of the gyroklystrons. Some of the milestones in the understanding of the gyroklystron principle are: the development of the generalized single mode analysis based on the linear and non-linear approaches [5], point gap model, and development of a self-consistent simulation code [6-7].

In the present work, the single mode generalized theory for the fundamental harmonic mode operation of the gyroklystron [5] based on the linear approach has been extended to estimate and optimize its electronic efficiency. The efficiency contours, which are to be used for the initial design parameter selection of a gyroklystron, have been drawn. The possible operating regions are to be chosen from these contours by taking suitable normalized parameters, i.e., normalized field amplitude, beam current, interaction length and detuning parameter. These normalized parameters provide the complete specification of the beam parameter as well as structure parameter. These efficiency contours are generalized and used for designing a gyroklystron operating at any frequency and output power.

The developed analysis has been used further for calculating the efficiency of an experimental two cavity gyroklystron device reported in the literature [8]. The obtained analytical results are in close agreement with the reported experimental values.

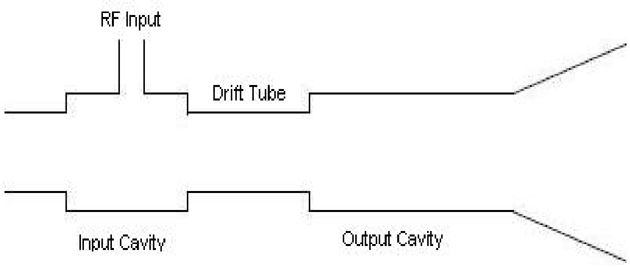

Figure 1: Schematic of a two-cavity gyroklystron

2. ANALYSIS

Considering the interaction of the relativistic electron beam with the RF electromagnetic field inside a two-cavity gyroklystron (figure 1) the equations of motion of the electrons can be obtained. The space–charge effect is assumed to be negligibly small and the effect of a velocity spread on beam wave interaction in the cavities can be neglected. For a single mode interaction and a weakly relativistic electron approximation { $(n\beta_\perp^2/2) << 1$, where n is the cyclotron harmonic number, the equations of motion for the electrons reduces to the pendulum equations also known as the Yulpatov equations [5], and can be written as:

$$\frac{dp}{d\xi} = -Ff(\xi)(p)^{n-1}\sin(\theta) \quad , \qquad (1)$$

$$\frac{d\theta}{d\xi} = (\Delta + p^2 - 1) - nFf(\xi)(p)^{n-2}\cos(\theta) \quad , \qquad (2)$$

where p, θ_0 and ξ are the normalized momentum, electron phase and normalized axial position, respectively. These are the two working equations for the gyroklystron with $p(\xi_{in}) = 1$ and $\theta(\xi_{in}) = \theta_0$, where θ_0 is uniformly distributed over [0,2π]. Here, we have chosen $\xi_{in} = -\sqrt{3}\,\mu/2$ and $\xi_{out} = \sqrt{3}\,\mu/2$ as the normalized input and output lengths for the output cavity as they are a good approximation to the actual gyroklystron output cavity. The function $f(\xi)$ in equations (1) and (2) are chosen to be a Gaussian field profile given by:

$$f(\xi) = e^{-(2\xi/\mu)2} \quad . \qquad (3)$$

For a given initial distribution of θ_0, the system is parameterized by the normalized field amplitude F, normalized interaction length μ and the detuning parameter Δ given by [6]:

$$F = \frac{E_0 \beta_{\perp 0}{}^{n-4}}{B_0 c}\left(\frac{n^{n-1}}{2^{n-1} n!}\right) J_{m\pm n}(k_\perp R_e) \qquad (4)$$

$$\mu = \frac{\pi \beta_{\perp 0}{}^2}{\beta_{\parallel 0}} \frac{L}{\lambda} \qquad (5)$$

$$\Delta = \frac{2}{\beta_{\perp 0}{}^2}\left(1 - \frac{n\omega_{c0}}{\omega}\right) \qquad (6)$$

where L is the length of the cavity and R_e is the beam radial position. The electric field amplitude E_0 can be calculated as [10]:

$$E_0 = \sqrt{\frac{QP_{in}}{\omega \varepsilon_0 \pi L}} \frac{2}{R_0 \,|\, J_0(\upsilon_{0p}) \,|} \quad . \qquad (7)$$

Now in the light of above equations, electronic efficiency of gyroklystron in the absence of velocity spread can be obtained by taking an average over the initial phase angles θ_0 as

$$\eta = \frac{\beta_{\perp 0}^2}{2(1 - \gamma_0^{-1})}\left[1 - \left\langle p^2(\xi_{out})\right\rangle_{\theta_0}\right] \quad . \qquad (8)$$

To perform the analysis, we consider the case of a two cavity gyroklystron, i.e., first cavity as the prebuncher. Since F is small, the nonlinear pendulum equations given by equation (1) and (2) are integrated analytically by expanding p and θ in the small parameter F as follows:

$$\left.\begin{aligned} p &= p^{(0)} + p^{(1)} + \ldots \\ \theta &= \theta^{(0)} + \theta^{(1)} + \ldots \end{aligned}\right\} \quad . \qquad (9)$$

On inserting this expansion in equation (1) and (2) and considering $n = 1$,

$$\frac{dp^{(0)}}{d\xi} = 0 \qquad (10)$$

$$\frac{d\theta^{(0)}}{d\xi} = -\left(\Delta + p^{(0)^2} - 1\right) \qquad (11)$$

$$\frac{dp^{(1)}}{d\xi} = -Ff(\xi)\sin\theta^{(0)} \qquad (12)$$

$$\frac{d\theta^{(1)}}{d\xi} = -2p^{(0)}p^{(1)} - \frac{Ff(\xi)\cos(\theta^{(0)})}{p^{(0)}} \quad . \qquad (13)$$

The equations (10) and (11) describe the undisturbed state of the electron beam (when no RF field is applied). On integrating these equations we get:

$$p^{(0)}(\xi) = 1 \qquad (14)$$

$$\theta^{(0)}(\xi) = \theta_0 + \Delta(\xi_{in} - \xi) = \theta_c - \Delta\xi \quad , \qquad (15)$$

where θ_0 and θ_c are uniformly distributed over [0, 2π]. Now, equation (12) which describes the electron momentum modulation by the RF field is integrated using the field profile equation (3) and equation (15). This gives the electron momentum at the output of the first cavity approximated upto the first order in F as:

$$p_1(\xi_{out}) = p^{(0)}(\xi_{out}) + p^{(1)}(\xi_{out}) = 1 - (\sqrt{\pi}/2) F\mu G(x)\sin\theta_c \quad . \tag{16}$$

Similarly, equation (13) describing the bunching of the electron phase angles is integrated and added to equation (15). Thus, the electron phase angle at the output of the first cavity can be written as:

$$\theta(\xi_{out}) = \theta_c - \sqrt{3}/2\,\mu\Delta + \sqrt{\pi}/2\,F\mu e^{-x^2}\left\{\sqrt{3}\mu\sin\theta_c + \mu x\cos\theta_c - \cos\theta_c\right\} \cdot \tag{17}$$

The first two terms within the brackets describes the inertial bunching, whereas the last term characterizes the force bunching. In most cases of interest, only first inertial term dominates since μ is usually larger than one and $|\mu x\text{-}1| << 1$ due to the requirement that the start oscillation current of the prebuncher cavity should be high in order to prevent self-oscillations.

After the first cavity, drift section is there where momentum p remains constant (since no RF field is excited) and is given by equation (16) and due to inertial bunching mechanism bunched phase angles θ will evolve as:

$$\frac{d\theta}{d\xi} = -\Delta_d + \sqrt{\pi}F_1\mu_1 e^{-x_1^2}\sin\theta_c \ , \tag{18}$$

where 1 and d are the quantities defined in the first cavity and drift section, respectively. The bunched phase angles at the end of the drift section is obtained by solving above equation with the initial condition specified by equation (17):

$$\theta_b = \theta_c - \left((\sqrt{3}/2)\mu_1\Delta_1 + \mu_d\Delta_d\right) + q\sin\theta_c \quad , \tag{19}$$

where μ_b is the drift length and q is defined as the bunching parameter and is given by:

$$q = \sqrt{\pi}F_1\mu_1 e^{-x_1^2}\left((\sqrt{3}/2)\mu_1 + \mu_d\right) \ . \tag{20}$$

As a result, the electron phase angles, at the input of the second cavity can be parameterized by the bunching parameter q and the constant phase ψ which is the phase difference between the cavities and the electron rotational drift, as:

$$\theta_{0,2} = \theta_c + q\sin\theta_c - \psi \quad , \tag{21}$$

$$\psi = (\sqrt{3}/2)\mu_1\Delta_1 + \mu_d\Delta_d \quad . \tag{22}$$

By solving the linearized equations with the initial conditions given by equation (16) and (21) in the second cavity, one can calculate the small-signal efficiency of the device. Again, on solving the linearized equations with the initial conditions given by equation (16) and (21) up to the first order in F_1 and F_2, the transverse momentum at the output of the second cavity is calculated and can be given as:

$$p_2(\xi_{out}) = 1 - (\sqrt{\pi}/2)F_1\mu_1 e^{-x_1^2}\sin\theta_c - (\sqrt{\pi}/2)F_2\mu_2 e^{-x_2^2}\sin\left[\theta_{0,2} - (\sqrt{3}/2)\mu_2\Delta_2\right] \cdot \tag{23}$$

The expression for the orbital efficiency which is necessary for calculating the electronic efficiency of gyroklystron is obtained by performing an average over the initial phase angles θ_0 and can be written as:

$$\eta_\perp^{lin} = 1 - \left\langle p_2^2(\xi_{out})\right\rangle_{\theta_o} \quad . \tag{24}$$

In the output cavity of the gyroklystron, the range of integration is taken as $-\sqrt{3}\mu/2 \le \varsigma \le \sqrt{3}\mu/2$. By using equations (21), (23), and (24), we can obtain the relation for the electronic efficiency as:

$$\eta = \sqrt{\pi}/2\,F_2\mu_2 e^{-x_2^2} J_1(q)\sin\left(\psi + (\sqrt{3}/2)\mu_2\Delta_2\right)\left(\frac{\beta_{\perp 0}^2}{\left(1-\gamma_0^{-1}\right)}\right) \quad , \tag{25}$$

where F_2 is the normalized field amplitude at the output of the second cavity and can be given as [7]:

$$F_2 = \sqrt{\pi}I_2\mu_2 e^{-(\mu_2\Delta_2/4)^2} J_1(q)\left(\sin\psi + \frac{\mu_2^2\Delta_2/4 - 1}{(\sqrt{3}/2)\mu_1 + \mu_d}\cos\psi\right) \cdot \tag{26}$$

In equation (26) I_2 is the normalized beam current given by:

$$I_2 = \left(\frac{2}{\pi^5}\right)^{1/2}\frac{I_0 Qe}{c^3 m_e\varepsilon_0}\frac{\beta_{\perp 0}{}^{-4}}{\gamma_0}\frac{\lambda}{L_2}\frac{J^2_{m\pm n}(k_\perp R_e)}{(\upsilon_{mp}{}^2 - m^2)J_m{}^2(\upsilon_{mp})} \quad . \tag{27}$$

Here, I_0 is the beam current in amperes, Q is the loaded quality factor and L_2 is the length of the output cavity. If I_2 and F_2 are known, the transverse efficiency can also be obtained by using power balance equation as:

$$\eta_\perp I_2 = F_2^2 \quad . \tag{28}$$

3. RESULTS AND DISCUSSION

The orbital efficiency of the gyroklystron is defined as the average electron energy loss from their initial transverse energy. The orbital efficiency is calculated numerically from electron motion and RF field quantity. Once the orbital efficiency is estimated, the electronic efficiency of the device which is defined as the conversion of DC beam power to RF output power and calculated using equation (25). It can be seen from equation (25) that the orbital efficiency along with the electronic efficiency of a gyroklystron amplifier depends on five parameters, normalized field amplitude F, normalized interaction length μ, detuning parameter Δ, bunching parameter q and constant electron phase ψ. Thus, on optimizing all these parameters, the maximum efficiency is obtained. The parameters, are optimized as $\Delta = 0$, $q = 1.85$ and $\psi = \pi/2$, for fundamental harmonic operation ($n = 1$). On varying the normalized field amplitude F_2 and normalized interaction length μ_2, the contour plot of transverse efficiency as a function of normalized field amplitude (F_2) and normalized length (μ_2) is obtained (figure 2). As seen in figure 2, the maximum transverse efficiency is obtained around 70% at $F_2 = 0.05$ and $\mu_2=14$. Using the power balance equation (28), the contour plot of transverse efficiency as a function of normalized beam current I_2 and normalized interaction length μ_2 is plotted (figure 3). As seen in figure 3, the maximum transverse efficiency is obtained around 70 % at $\mu_2=14$ and $I_2 = 0.0045$. The contour plots obtained here are used for the efficiency estimation of a experimentally reported typical two cavity fundamental harmonic gyroklystron.

Table 1: Design Specifications for 35 GHz, 200 kW two-cavity gyroklystron [8]

Parameters	**Specifications**
Beam Voltage	70 kV
Beam Current	8.2 A
Velocity Pitch Factor	1.43
Operating Mode	TE_{01}
Center Frequency	34.95 GHz
DC Magnetic Field	1.31T
Input Cavity Length	1.5λ
Output Cavity Length	2.75 λ
Input Cavity Radius	5.6 mm
Output Cavity Radius	5.35 mm
Drift Tube Length	1.7λ
Drift Tube Radius	4.1 mm

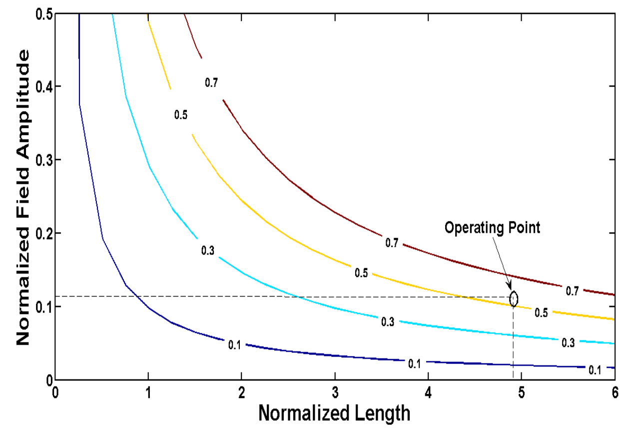

Figure 2: Contour plot of linear transverse efficiency as a function of normalized field amplitude and normalized length

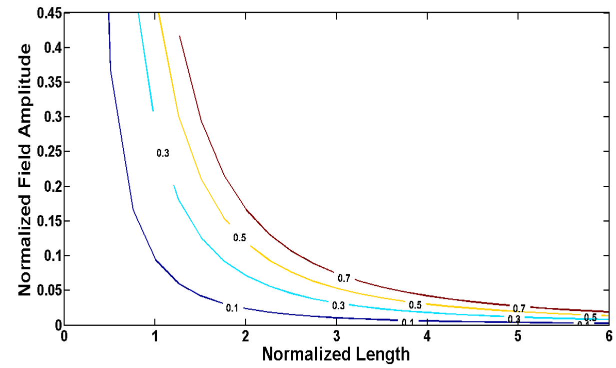

Figure 3: Contour plot of linear transverse efficiency as a function of normalized beam current and normalized length

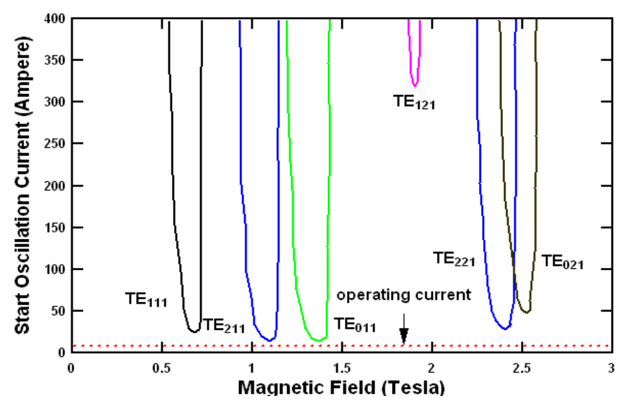

Figure 4: Start oscillation current for different modes as a function of magnetic field

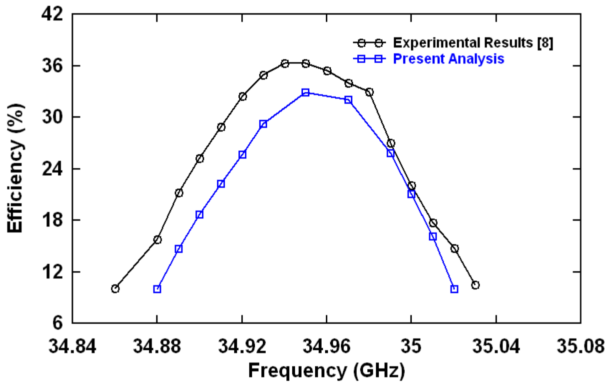

Figure 5: Efficiency as a function of frequency

The analysis of 35 GHz, 200 kW fundamental harmonic two-cavity gyroklystron with all the cavities operating in the TE_{01} mode has been carried out using the approach developed above. Table 1 shows the design specifications taken for analysis of 35 GHz, 200 kW two cavity gyroklystron. The operating point of the gyroklystron has been chosen with the help of the efficiency contour corresponding to its normalized output cavity length as shown in figure 2. The electronic efficiency of the device under consideration is calculated by using equation (25). The electronic efficiency as estimated by the contour plots is 32.8% and the reported efficiency is 36.2%. The start oscillation current (figure 4 is calculated for TE_{01} mode for 35 GHz gyroklystron with respect to magnetic field B_0 and it is observed that the start oscillation current I_{st} is obtained as around 12 A which is greater than the operating current 8.2 A, thus ensuring the stable operation of gyroklystron as an amplifier. The analysis has been further used to study the effect of variation of frequency on efficiency (figure 5). It is clear from figure 5 the maximum efficiency is obtained around 32.8% at center frequency 34.95 GHz. The analytical results obtained here are validated with the help of reported experimental results [8].

4. CONCLUSION

The electronic efficiency estimation and optimization for gyroklystron has been performed using single mode linear analysis. The efficiency contour plots needed for the design of a gyroklystron operating at the fundamental harmonic mode has been drawn. The electronic efficiency of a typical two cavity Ka band gyroklystron experimentally reported in the literature, has been estimated using these developed contour plots. The analytical results obtained here have been validated with the published experimental results. The analytical results are in agreement with the reported experimental values within ~10%. The efficiency contours obtained from the present analysis are generalized in nature. Therefore, it can be concluded that the present analysis will be helpful in the preliminary design of the gyroklystrons amplifiers.

5. ACKNOWLEDGEMENT

One of the authors (Madan Singh Chauhan) is thankful to Centre of Advanced Studies (University Grant Commission), Department of Electronics Engineering, IIT (BHU), for financial support.

REFERENCES

1. Steven H. Gold and Gregory S. Nusinovich. **Review of high-power microwave source research**, *Review of Scientific Instruments*, Vol. 68, pp. 3945-3974, 1997.
2. V. L. Granatstein and W. Lawson. **Gyro-amplifiers as candidate RF drivers for TeV linear colliders,** *IEEE Trans. Plasma Sci*., Vol. 24, pp. 648–665, 1996.
3. Manfred Thumm. **Novel applications of millimeter and sub-millimeter wave gyro-devices**, *International Journal of Infrared and Millimeter Waves,* Vol. 22, pp. 377-386, 2001.
4. H. Henke. **Millimeter-wave structures and power sources,** *Proceedings of European particle accelerator conference*, pp. 202-206, Vienna, Austria, 2000.
5. T. M. Tran, B. G. Danly, K. E. Kreischer, J. B. Schutkeker and R. J. Temkin. **Optimization of gyroklystron efficiency,** *Physics of Fluids*, Vol. 29, pp. 1274-1281, 1986.
6. G. S. Nusinovich. ***Introduction to the physics of gyrotrons,*** Baltimore, Maryland: Johns Hopkins Univ. Press, 2004.
7. Zhi-Hui Geng and Pu-Kun Liu. **Calculation of the electron efficiency for a two-cavity gyroklystron amplifier by using a self-consistent code**, *International Journal of Infrared and Millimeter Waves,* Vol. 25, pp. 1133-1141, 2004.
8. Jin Joo Choi, Alan H. McCurdy, F. N. Wood, R. H. Kyser, J. P. Calame, Khanh T. Nguyen, **Experimental investigation of a high Power, two-cavity, 35 GHz gyroklystron amplifier**, *IEEE Transactions on Plasma Science*, Vol. 26, pp. 416-425, 1998.
9. O. Dumbrajs, R. Meyer-Spasche and A. Reinfelds, **Analysis of electron trajectories in a gyrotron resonator,** *IEEE Trans. Plasma Sci.,* Vol. 26, pp. 846-852, 1998.
10. C. D. Joye, M. A. Shapiro, R. J. Sirigiri, R. J. Temkin. **Design of a 140 GHz, 100 W gyroklystron amplifier,** *IEEE Int. Vacuum Electronic Conference*, Monterey, US, pp. 198-199, 2004.